

## Interaction between $V_2O_5$ nanowires and high pressure $CO_2$ gas up to 45 bar: Electrical and structural study



Hyun-Seok Jang<sup>a,b,c,1</sup>, Chang Yeon Lee<sup>d,1</sup>, Jun Woo Jeon<sup>a,b,c</sup>, Won Taek Jung<sup>a,b,c</sup>, Junyoung Mun<sup>d</sup>,  
Byung Hoon Kim<sup>a,b,c,\*</sup>

<sup>a</sup> Department of Physics, Incheon National University, 22012 Incheon, Republic of Korea

<sup>b</sup> Institute of Basic Science, Incheon National University, 22012 Incheon, Republic of Korea

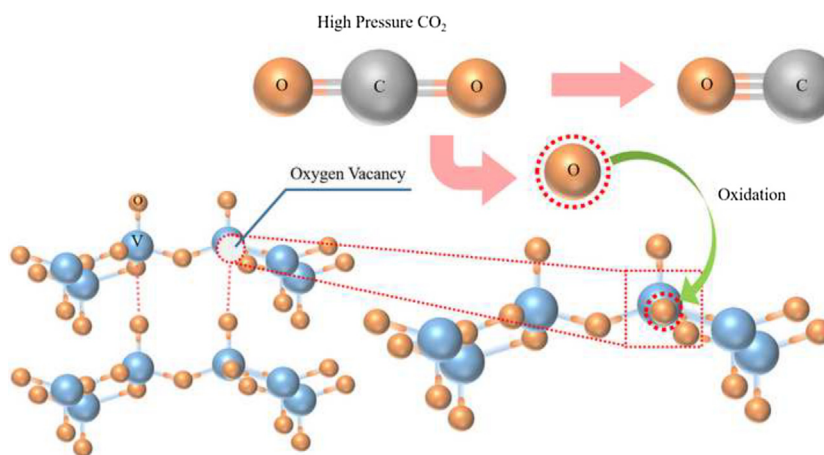
<sup>c</sup> Intelligent Sensor Convergence Research Center, Incheon National University, 22012, Incheon, Republic of Korea

<sup>d</sup> Department of Energy and Chemical Engineering, Incheon National University, Incheon 22012, Republic of Korea

### HIGHLIGHTS

- $CO_2$  gas pressure-dependent conductance ( $G(P)$ ) of vanadium-oxides nanowires (VON) from vacuum to 45 bar decreases with the increase of the gas pressure.
- Increase in the interlayer distance and decrease in phonons for  $V_3-O$  and  $V-O-V$  bonds were observed after high  $CO_2$  pressure exposure.
- Oxidation of  $V^{4+}$  to  $V^{5+}$  due to high  $CO_2$  pressure is the reason for these changes.
- Oxidative dehydrogenation process with VON catalyst under high pressure  $CO_2$  atmosphere has potential to improve the efficiency.

### GRAPHICAL ABSTRACT



### ARTICLE INFO

#### Article history:

Received 31 October 2019

Revised 23 January 2020

Accepted 27 January 2020

Available online 30 January 2020

#### Keywords:

Carbon dioxide

High  $CO_2$  pressure

Oxidative dehydrogenation

$V_2O_5$  Nanowire

### ABSTRACT

In the oxidative dehydrogenation (ODH) process that converts ethylbenzene to styrene, vanadium-based catalysts, especially  $V_2O_5$ , are used in a  $CO_2$  atmosphere to enhance process efficiency. Here we demonstrate that the activation energy of  $V_2O_5$  can be manipulated by exposure to high pressure  $CO_2$ , using  $V_2O_5$  nanowires (VON). The oxidation of  $V^{4+}$  to  $V^{5+}$  was observed by X-ray photoelectron spectroscopy. The ratio of  $V^{4+}/V^{5+}$  which the typical comparable feature decreased 73.42%. We also found an increase in the interlayer distance in VON from 9.95 Å to 10.10 Å using X-ray diffraction patterns. We observed changes in the peaks of the stretching mode of bridging triply coordinated oxygen ( $V_3-O$ ), and the bending vibration of the bridging  $V-O-V$ , using Raman spectroscopy. We confirmed this propensity by measuring the  $CO_2$  pressure-dependent conductance of VON, up to 45 bar. 92.52% of decrease in the maximum conductance compared with that of the pristine VON was observed. The results of this study suggest that ODH process performance can be improved using the VON catalyst in a high pressure  $CO_2$  atmosphere.

© 2020 THE AUTHORS. Published by Elsevier BV on behalf of Cairo University. This is an open access article under the CC BY-NC-ND license (<http://creativecommons.org/licenses/by-nc-nd/4.0/>).

Peer review under responsibility of Cairo University.

\* Corresponding author at: Department of Physics, Incheon National University, 22012 Incheon, Republic of Korea.

E-mail address: [kbh37@inu.ac.kr](mailto:kbh37@inu.ac.kr) (B.H. Kim).

<sup>1</sup> Hyun-Seok Jang and Chang Yeon Lee contributed equally to this work.

<https://doi.org/10.1016/j.jare.2020.01.014>

2090-1232/© 2020 THE AUTHORS. Published by Elsevier BV on behalf of Cairo University.

This is an open access article under the CC BY-NC-ND license (<http://creativecommons.org/licenses/by-nc-nd/4.0/>).

## Introduction

Carbon is the most fundamental element in ecological systems and biological organisms. The atmospheric concentration of carbon gas, particularly carbon dioxide ( $\text{CO}_2$ ), is also known to be the one of the main factors driving climate change, global warming and ocean acidification. Nevertheless,  $\text{CO}_2$  gas is widely used in industry, especially for styrene production.

Styrene is a mainstay material in the polymer industry. It is mostly produced using ethylbenzene via the oxidative dehydrogenation (ODH) process with a transition metal oxide [1–7]. Under the presence of inorganic oxidants, such as metal oxides reported in the last decades, the ODH process of organic aromatic compounds is accelerated [8–11]. Among various metal oxides, vanadium-based catalysts with various support materials have been focused because of their good catalytic performance, particularly styrene yields and selectivity [12–20]. In ODH using a vanadium-based catalyst, especially  $\text{V}_2\text{O}_5$ , the valence state of the vanadium switches back and forth between  $\text{V}^{4+}$  and  $\text{V}^{5+}$  as shown in Fig. 1 [21,22]. However, the persistent reduction of  $\text{V}^{5+}$  to  $\text{V}^{4+}$  results in catalyst deactivation. In other words, a large amount of  $\text{V}^{5+}$  compared with that of  $\text{V}^{4+}$  enhances the activation process.

A large amount of superheated steam has generally been used in the process as an oxidant, but in recent years,  $\text{CO}_2$  gas has become the preferred alternative oxidant, due to its advantages [1–7,12–20]. For example, in a  $\text{CO}_2$  atmosphere the latent heat is maintained throughout the entire reaction process [23] and there is a greater decrease in the partial pressure of the reactants with  $\text{CO}_2$  than with superheated steam [24]. This is the reason for the growing industrial interest in  $\text{CO}_2$  gas mentioned above.

It has been reported that high gas pressure can lower the dissociation energy of the gas, resulting in the modulation of the physical and electronic properties of 2D materials [25–30]. This suggests that high gas pressure can enhance the catalytic effect. Moreover, if small sized  $\text{V}_2\text{O}_5$  is used as a catalyst, it is expected that the ODH reaction will be reinforced because of the increase in surface area.

In this study, we synthesized  $\text{V}_2\text{O}_5$  nanowires (VON) and investigated their structural modulation and electrical transport property as a function of  $\text{CO}_2$  gas pressure from vacuum to 45 bar. The pressure-dependent Transconductance ( $G(P)$ ) decreased as the pressure increased, due to oxidation of the VON. This behavior was clarified by x-ray photoelectron spectroscopy (XPS), and structural changes were studied by x-ray diffraction (XRD) pattern and Raman spectroscopy before and after exposure to high pressure  $\text{CO}_2$ . We found an increase in the interlayer distance in the VON,

and an increase in the  $\text{V}^{5+}$  state, after the VON were exposed to high  $\text{CO}_2$  pressure. From the results in this study, we suggest that an ODH process with a VON catalyst can be improved by high-pressure  $\text{CO}_2$  atmosphere.

## Experimental

### Synthesis of the $\text{V}_2\text{O}_5$ nanowires

The VON was synthesized using a sol-gel method involving the polycondensation of vanadic acid in water [31]. VONs were synthesized from 5 g ammonium *meta*-vanadate (Aldrich) and 50 g acidic ion-exchange resin (DOWEX 50WX8-100, Aldrich) in 1 L deionized water, and then the mixture was kept at room temperature to produce an orange sol that darkened with time.

### Measurement electrical transport property of VON with respect to $\text{CO}_2$ gas pressure

Sol-gel based VON film was synthesized with VON by drying at  $80^\circ\text{C}$  for 48 h in an atmospheric condition. The dried VON film was cut into  $1 \times 5$  mm sections, and attached to an insulating substrate to measure its electrical conductance as a function of  $\text{CO}_2$  gas pressure using a home-made pressure chamber.

The VON film in the pressure chamber was heated at  $80^\circ\text{C}$  and high vacuum condition ( $1.0 \times 10^{-6}$  Torr) for 3 h to remove residues. After annealing, the VON film was cooled down to 300 K ( $300.00 \text{ K} \pm 0.20 \text{ K}$ ) and the temperature was maintained during the entire measurement process.

In this study, 99.999%  $\text{CO}_2$  gas was used.  $\text{CO}_2$  pressure was increased by 5 bar up to 45 bar.  $G(P)$  was measured 30 min after reaching each target pressure.  $G(P)$  was fitted from the  $I$ - $V$  curve of the VON film (the applied voltage was from  $-200$  mV to  $200$  mV, in 2 mV steps using a KEITHLEY SCS-4200, U.S.A.).

### Characterization of VON and $\text{CO}_2$ -VON

The morphology of the VON was observed using a scanning electron microscope (SEM, JEOL, JSM-7800F, Japan). The chemical species and structure of the VON and  $\text{CO}_2$ -VON were investigated by Raman spectroscopy (Witec, Alpha-300, Germany), X-ray photoelectron spectroscopy (XPS, ULVAC, PHI-5000 VersaProbe II, Japan), and X-ray diffraction (XRD, Rigaku, SmartLab HR-XRD, Japan).

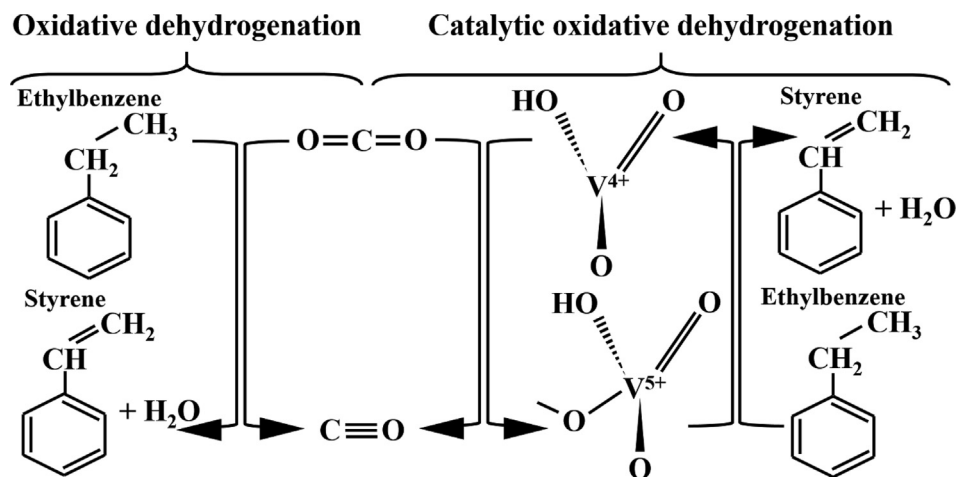


Fig. 1. Schematic for the mechanism of the ODH process of ethylbenzene with and without the presence of  $\text{V}_2\text{O}_5$  as a catalyst.

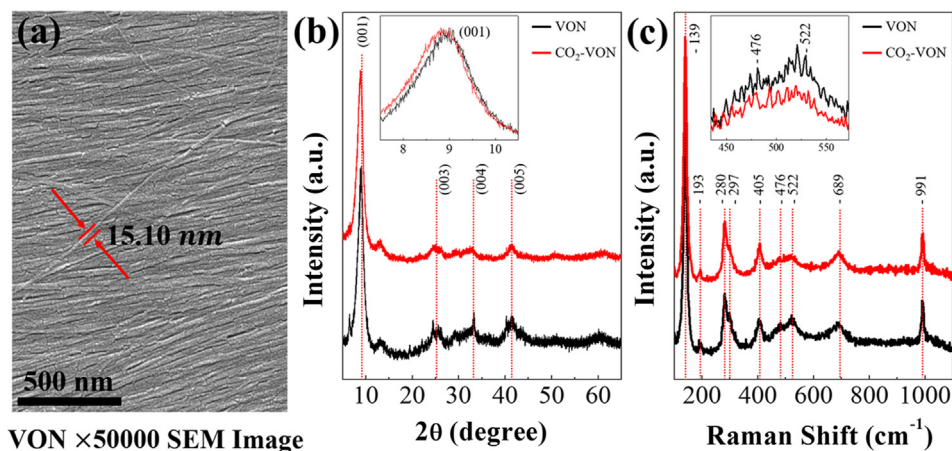


Fig. 2. (a) SEM Image of VON and (b) X-ray diffraction patterns and (c) Raman spectroscopy of VON and CO<sub>2</sub>-VON.

## Results and discussion

### Morphology and structural investigation with SEM, XRD, and Raman spectroscopy

Fig. 2(a) shows the SEM image of the VON. VON with diameters of about 10–20 nm, which is well consistent with the previous literatures [31–33]. The normalized XRD patterns of pristine VON and VON after high-pressure CO<sub>2</sub> gas exposure (CO<sub>2</sub>-VON) are shown in Fig. 2(b). The (0 0 1) peak of the CO<sub>2</sub>-VON has shifted to a smaller angle ( $2\theta = 8.88^\circ$  for VON and to  $8.75^\circ$  for CO<sub>2</sub>-VON, the inset of Fig. 2(b)), which indicates that the interlayer distance of the VON increased from 9.95 to 10.10 Å after CO<sub>2</sub> exposure. In order to confirm the structural modulation, Raman spectroscopy was performed.

Fig. 2(c) shows the normalized Raman peaks. The characteristic VON peaks were found [34–36]. The dominant peaks at 139 and 193 cm<sup>-1</sup> originate from the relative motions of two V<sub>2</sub>O<sub>5</sub> units belonging to the unit cell. The peaks at 280 and 405 cm<sup>-1</sup> are associated with the bending vibration of the V=O bonds. The peaks at 689 and 991 cm<sup>-1</sup>, respectively, correspond to the bending vibration of doubly coordinated oxygen (V<sub>2</sub>-O) and the stretching vibration mode of the shortest V-O<sub>1</sub>. These six peaks did not change even after high CO<sub>2</sub> pressure exposure. The peaks at 297, 522, and 476 cm<sup>-1</sup> were assigned to the bending vibration, the stretching mode of the bridging triply coordinated oxygen (V<sub>3</sub>-O), and the bending vibration of the bridging V-O-V, respectively. Although the peak intensity changed little, these three peaks were reduced after VON exposure to high CO<sub>2</sub> gas pressure (see Fig. S1 in Supplementary Information and the inset in Fig. 2(c)). This can be interpreted as follows. The amount of V-O-V and V<sub>3</sub>-O bonds is relatively small due to oxygen vacancies in the pristine VON. After CO<sub>2</sub> exposure, the VON is oxidized. As a result, the amplitude of vibration in both bonds (phonon) is weakened. This effect can be seen in  $G(P)$ .

### Electrical transport property of VON with respect to CO<sub>2</sub> gas pressure

Fig. 3 shows the electrical transport property of VON as a function of CO<sub>2</sub> gas pressure from vacuum ( $\sim 10^{-6}$  Torr) to 45 bar. As soon as the VON was exposed to 5 bar of CO<sub>2</sub> gas, the  $G(P)$  of the VON dramatically decreased from 26.33 to 13.92 μA, and then it gradually declined down to 1.97 μA at 45 bar of CO<sub>2</sub> pressure. This behavior is similar to the oxygen pressure-dependent conductance of VON [37].

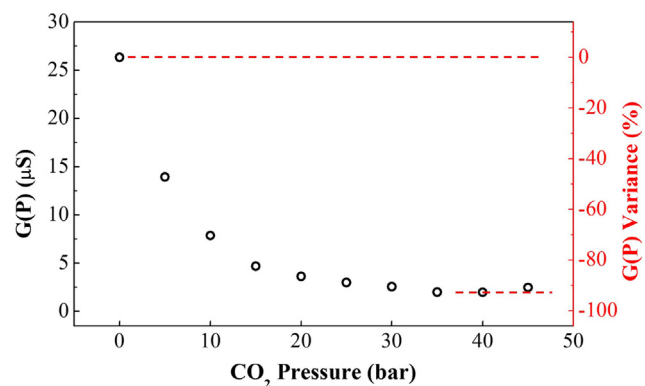


Fig. 3. CO<sub>2</sub>-Pressure dependent  $G(P)$  of VON from vacuum to 45 bar.

In general, charge transport in VON has been interpreted to be by small polaron hopping. The concentration ratio of V<sup>4+</sup>/(V<sup>4+</sup> + V<sup>5+</sup>) plays an important role in this transport behavior [25]. Specifically, the amount of V<sup>4+</sup> and V<sup>5+</sup> significantly affects the charge transport property, which is related to oxygen vacancies. It is well known that the charge carrier density in VON is proportional to the density of oxygen vacancies. Oxygen vacancies cause the reduction of V<sup>5+</sup>, producing V<sup>4+</sup>, which can be understood as V<sup>5+</sup> plus an additional electron [38]. This means that the electrical conductance of VON decreases when oxygen vacancies are reduced.

### X-ray photoelectron study before and after CO<sub>2</sub> exposure

For this reason, the valence state of the vanadium in VON before and after exposure to CO<sub>2</sub> was studied using XPS (Fig. 4). The surveys of pristine VON and CO<sub>2</sub>-VON are depicted in Fig. S2 in the Supplementary Information. Vanadium, oxygen, and carbon species were observed. The carbon peak in the pristine originates from the carbon tape used to support the sample, so we did not consider this peak. The peaks at approximately 530, 524, and 517 eV correspond to O 1s, V 2p<sub>1/2</sub>, and V 2p<sub>3/2</sub> (Fig. 4). The O1s peak consisted of three sub-peaks: V-OH at 533.29 eV, V-O-V at 531.65 eV, and O<sup>2+</sup> at 530.29 eV. The amount of V-OH slightly increased after CO<sub>2</sub> exposure (Table 1). This shows that the surface OH rarely changes after annealing and CO<sub>2</sub> exposure.

On the other hand, the amount of V-O-V bonds in the VON after CO<sub>2</sub> exposure increased from 37.07 to 54.61%. V<sub>2</sub>O<sub>3</sub>, V<sub>2</sub>O<sub>5</sub> (V<sup>5+</sup>), and VO<sub>2</sub> (V<sup>4+</sup>) species were observed in V 2p<sub>3/2</sub>. Note that the amount of V<sub>2</sub>O<sub>5</sub> species significantly increased from 48.05%

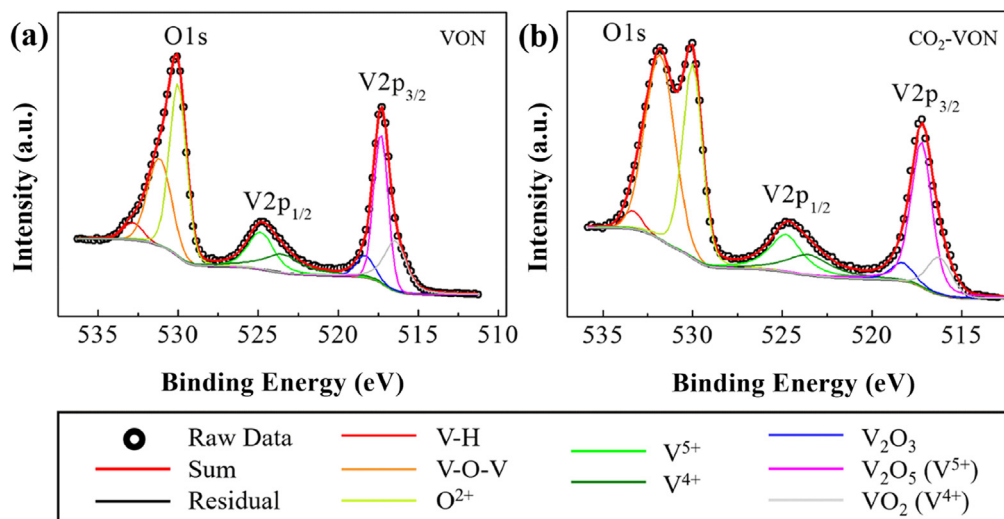


Fig. 4. X-ray photoelectron spectroscopy showing the O1s peak, V 2p<sub>1/2</sub> peak, and V 2p<sub>3/2</sub> peak in (a) VON and (b) CO<sub>2</sub>-VON.

Table 1

Atomic concentration in VON and CO<sub>2</sub>-VON obtained from the XPS results.

Peak List and chemical species (Position/ln-region ratio)	VON		CO <sub>2</sub> -VON		
<b>O1s</b>	<b>V-OH</b>	533.29 / 1.69%	42.29%	533.33/3.34%	56.05%
	<b>V-O-V</b>	531.62/11.76%		531.82/54.61%	
	<b>O<sup>2+</sup></b>	530.29/86.54%		530.00/42.05%	
<b>V2p<sub>1/2</sub></b>	<b>V<sup>5+</sup></b>	524.80/26.99%	19.71%	524.82/57.26%	16.27%
	<b>V<sup>4+</sup></b>	523.70/73.01%		523.65/42.72%	
<b>V2p<sub>3/2</sub></b>	<b>V<sub>2</sub>O<sub>3</sub></b>	518.03/6.23%	38.00%	518.31/9.94%	27.64%
	<b>V<sub>2</sub>O<sub>5</sub>(V<sup>5+</sup>)</b>	517.16/48.05%		517.24/71.89%	
	<b>VO<sub>2</sub>(V<sup>4+</sup>)</b>	516.27/45.72%		516.25/18.18%	

for VON, to 71.89% for CO<sub>2</sub>-VON, but the VO<sub>2</sub> species decreased from 45.72% to 18.18%.

Since the charge transport in VON is mainly governed by the amount of V<sup>4+</sup> and V<sup>5+</sup> as mentioned above, we focused on the vanadium species. The ratio of V<sup>4+</sup>/V<sup>5+</sup> changed from 0.952 for the pristine VON to 0.253 for CO<sub>2</sub>-VON. The decrease in V<sup>4+</sup>/V<sup>5+</sup> in the VON after CO<sub>2</sub> exposure indicates that the VON was oxidized due to CO<sub>2</sub>. A notable point is that *G*(*P*) continuously decreased and saturated with the increase in CO<sub>2</sub> pressure. This means that the high CO<sub>2</sub> pressure enhanced the oxidation of the reduced VON.

## Conclusions

This study investigated the effect of high CO<sub>2</sub> gas pressure on VON conductivity, and revealed that pressure-dependent oxidation intrinsically reduced the VON. *G*(*P*) continuously decreased as CO<sub>2</sub> pressure increased, which resulted in an increase in V<sup>5+</sup>. This behavior was confirmed by XPS taken before and after exposure to high CO<sub>2</sub> pressure. Upon CO<sub>2</sub> gas exposure, the ratio of V<sup>4+</sup>/V<sup>5+</sup> was reduced by four times. Structural modulation resulting from CO<sub>2</sub> gas exposure was also studied by XRD and Raman spectroscopy. The interlayer distance in the VON increased from 9.95 to 10.10 Å, due to an increase in the amount of V—O—V and V<sub>3</sub>—O bonds. This study provides a potential method for improving the ODH process using a VON catalyst in a high-pressure CO<sub>2</sub> atmosphere.

## Ethics statement

This article does not contain any studies with human or animal subjects.

## Acknowledgement

This work was supported by the Incheon National University Research Grant in 2016–2328 and Basic Science Research Program through the National Research Foundation of Korea (NRF) funded by the Ministry of Education (NRF-2017R1A1A1A05000789).

## Declaration of Competing Interest

The authors declare no conflict of interest.

## Appendix A. Supplementary data

Supplementary data to this article can be found online at <https://doi.org/10.1016/j.jare.2020.01.014>.

## References

- [1] Li X, Feng J, Fan H, Wang Q, Li W. The dehydrogenation of ethylbenzene with CO<sub>2</sub> over Ce<sub>x</sub>Zr<sub>1-x</sub>O<sub>2</sub> solid Solutions. *Catal. Commun.* 2015;59:104–7.
- [2] Burri A, Jiang N, Yahyaoui K, Park S-E. Ethylbenzene to styrene over alkali doped TiO<sub>2</sub>-ZrO<sub>2</sub> with CO<sub>2</sub> as soft oxidant. *Appl. Catal. A: Gen.* 2015;495:192–9.
- [3] Wang T, Guan X, Lu H, Liu Z, Ji M. Nanoflake-assembled Al<sub>2</sub>O<sub>3</sub>-supported CeO<sub>2</sub>-ZrO<sub>2</sub> as an efficient catalyst for oxidative dehydrogenation of ethylbenzene with CO<sub>2</sub>. *Appl. Surf. Sci.* 2017;398:1–8.
- [4] Wang C, Shi J, Cui X, Zhang J, Zhang C, Wang L, et al. The role of CO<sub>2</sub> in dehydrogenation of ethylbenzene over pure α-Fe<sub>2</sub>O<sub>3</sub> catalysts with different facets. *J. Catal.* 2017;345:104–12.
- [5] Wang T, Qi L, Lu H, Ji Min. Flower-like Al<sub>2</sub>O<sub>3</sub>-supported iron oxides as an efficient catalyst for oxidative dehydrogenation of ethylbenzene with CO<sub>2</sub>. *J. CO<sub>2</sub> Util.* 2017;17:162–9.

- [6] Wang T, Chong S, Wang T, Lu H, Min Ji. The physicochemical properties and catalytic performance of carbon-covered alumina for oxidative dehydrogenation of ethylbenzene with CO<sub>2</sub>. *Appl. Surf. Sci.* 2018;427:1011–8.
- [7] Wang H, Yang G-Q, Song Y-H, Liu Z-T, Liu Z-W. Defect-rich Ce<sub>1-x</sub>Zr<sub>x</sub>O<sub>2</sub> solid solutions for oxidative dehydrogenation of ethylbenzene with CO<sub>2</sub>. *Catal. Today* 2019;324:39–48.
- [8] Li XG, Liao Y, Huang MR, Strong V, Kaner RB. Ultra-sensitive chemosensors for Fe (III) and explosives based on highly fluorescent oligofluoranthene. *Chem. Sci.* 2013;4(5):1970–8.
- [9] Li XG, Liao Y, Huang MR, Kaner RB. Interfacial chemical oxidative synthesis of multifunctional polyfluoranthene. *Chem. Sci.* 2015;6(3):2087–101.
- [10] Li XG, Liao Y, Huang MR, Kaner RB. Efficient synthesis of oligofluoranthene nanorods with tunable functionalities. *Chem. Sci.* 2015;6(12):7190–200.
- [11] Li XG, Liu YW, Huang MR, Peng S, Gong LZ, Moloney MG. Simple efficient synthesis of strongly luminescent polypyrene with intrinsic conductivity and high carbon yield by chemical oxidative polymerization of pyrene. *Chem.–A Eur. J.* 2010;16(16):4803–13.
- [12] Sakurai Y, Suzuki T, Ikenaga N-O, Suzuki T. Dehydrogenation of ethylbenzene with an activated carbon-supported vanadium catalyst. *Appl. Catal. A: Gen.* 2000;192:281–8.
- [13] Liu BS, Chang RZ, Jiang L, Liu W, Au CT. Preparation and high performance of La<sub>2</sub>O<sub>3</sub>-V<sub>2</sub>O<sub>5</sub>/MCM-41 catalysts for ethylbenzene dehydrogenation in the presence of CO<sub>2</sub>. *J. Phys. Chem. C* 2008;112:15490–501.
- [14] Rao KN, Reddy BM, Abhishek B, Seo Y-H, Jiang N, Park S-E. Effect of ceria on the structure and catalytic activity of V<sub>2</sub>O<sub>5</sub>/TiO<sub>2</sub>-ZrO<sub>2</sub> for oxidative dehydrogenation of ethylbenzene to styrene utilizing CO<sub>2</sub> as soft oxidant. *Appl. Catal. B: Environ.* 2009;91:649–56.
- [15] Wang C, Fan W-B, Liu Z-T, Lu J, Liu Z-W, Qin Z-F, et al. The dehydrogenation of ethylbenzene with CO<sub>2</sub> over V<sub>2</sub>O<sub>5</sub>/Ce<sub>x</sub>Zr<sub>1-x</sub>O<sub>2</sub> prepared with different methods. *J. Mol. Catal. A: Chem.* 2010;329:64–70.
- [16] Liu Z-W, Wang C, Fan W-B, Liu Z-T, Hao Q-Q, Long X, et al. V<sub>2</sub>O<sub>5</sub>/Ce<sub>0.6</sub>Zr<sub>0.4</sub>O<sub>2</sub>-Al<sub>2</sub>O<sub>3</sub> as an efficient catalyst for the oxidative dehydrogenation of ethylbenzene with carbon dioxide. *Chem. Sus. Chem.* 2011;4:341–5.
- [17] Chen S, Qin Z, Wang G, Dong M, Wang J. Promoting effect of carbon dioxide on the dehydrogenation of ethylbenzene over silica-supported vanadium catalysts. *Fuel* 2013;109:43–8.
- [18] Zhang S, Li X, Jing J, Fan H, Wang Q, Li W. Dehydrogenation of ethylbenzene with CO<sub>2</sub> over V<sub>2</sub>O<sub>5</sub>/Al<sub>2</sub>O<sub>3</sub>-ZrO<sub>2</sub> catalyst. *Catal. Commun.* 2013;34:5–10.
- [19] Fan H, Feng J, Li X, Guo Y, Li W, Xie K. Ethylbenzene dehydrogenation to styrene with CO<sub>2</sub> over V<sub>2</sub>O<sub>5</sub> (001): a periodic density functional theory study. *Chem. Eng. Sci.* 2015;135:403–11.
- [20] Betiha MA, Rabie AM, Elfadly AM, Yehia FZ. Microwave assisted synthesis of a VO<sub>x</sub>-modified disordered mesoporous silica for ethylbenzene dehydrogenation in presence of CO<sub>2</sub>. *Micropor. Mesopor. Mater.* 2016;222:44–54.
- [21] Kainthla I, Babu GVR, Bhanushali JT, Keri RS, Rao KSR, Nagaraja BM. Vapor-phase dehydrogenation of ethylbenzene to styrene over a V<sub>2</sub>O<sub>5</sub>/TiO<sub>2</sub>-Al<sub>2</sub>O<sub>3</sub> catalyst with CO<sub>2</sub>. *New J. Chem.* 2017;41(10):4173–81.
- [22] Zhao X, Yan Y, Mao L, Fu M, Zhao H, Sun L, et al. A relationship between the V<sup>4+</sup>/V<sup>5+</sup> ratio and the surface dispersion, surface acidity, and redox performance of V<sub>2</sub>O<sub>5</sub>-WO<sub>3</sub>/TiO<sub>2</sub> SCR catalysts. *RSC Adv.* 2018;8(54):31081–93.
- [23] Adams CR, Jennings TJ. Catalytic oxidations with sulfur dioxide: II. Alkylaromatics. *J. Catal.* 1970;17:157–77.
- [24] Chen S, Qin Z, Xu X, Wang J. Structure and properties of the alumina-supported vanadia catalysts for ethylbenzene dehydrogenation in the presence of carbon dioxide. *Appl. Catal. A: Gen.* 2006;302:185–92.
- [25] Kim BH, Hong SJ, Baek SJ, Jeong HY, Park N, Lee M, et al. N-type graphene induced by dissociative H<sub>2</sub> adsorption at room temperature. *Sci. Rep.* 2012;2:690.
- [26] Hong SJ, Park M, Kang H, Lee M, Soler-Delgado D, Shin DS, et al. Verification of electron doping in single-layer graphene due to H<sub>2</sub> exposure with thermoelectric power. *Appl. Phys. Lett.* 2015;106:142110.
- [27] Kim J, Kwak CH, Jung W, Huh YS, Kim BH. Variation in the c-axis conductivity of multi-layer graphene due to H<sub>2</sub> exposure. *Phys. Chem. Chem. Phys.* 2016;18:15514–8.
- [28] Hong SJ, Park M, Kang H, Lee M, Soler-Delgado D, Jeong DH, et al. Manipulation of electrical properties in CVD-grown twisted bilayer graphene induced by dissociative hydrogen adsorption. *Curr. Appl. Phys.* 2016;16:1637–41.
- [29] Hong SJ, Kim H, Lee M, Kang H, Park M, Jeong DH, et al. Chemical manipulation of edge-contact and encapsulated graphene by dissociated hydrogen adsorption. *RSC Adv.* 2017;7:6013–7.
- [30] Kang H, Hong SJ, Park M, Jang H-S, Nam K, Choi S, et al. Tuning the electronic structure of single-walled carbon nanotube by high-pressure H<sub>2</sub> exposure. *Nanotechnology.* 2018;30:065201.
- [31] Muster J, Kim GT, Krstić V, Park JG, Park YW, Roth S, et al. Electrical transport through individual vanadium pentoxide nanowires. *Adv. Mater.* 2000;12:420–4.
- [32] Chen Z, Qin Y, Weng D, Xiao Q, Peng Y, Wang X, et al. Design and synthesis of hierarchical nanowire composites for electrochemical energy storage. *Adv. Funct. Mater.* 2009;19:3420–6.
- [33] Xiong C, Aliev AE, Gnade B, Balkus Jr KJ. Fabrication of silver vanadium oxide and V<sub>2</sub>O<sub>5</sub> nanowires for electrochromics. *ACS Nano* 2008;2:293–301.
- [34] Baddour-Hadjean R, Raekelboom E, Pereira-Ramos JP. New structural characterization of the Li<sub>x</sub>V<sub>2</sub>O<sub>5</sub> system provided by Raman spectroscopy. *Chem. Mater.* 2006;18:3548–56.
- [35] Lee S-H, Cheong HM, Seong MJ, Liu P, Tracy CE, Mascarenhas A, et al. Microstructure study of amorphous vanadium oxide thin films using Raman spectroscopy. *J. Appl. Phys.* 2002;92:1893–7.
- [36] Kim BH, Yu HY, Hong WG, Park J, Jung SC, Nam Y, et al. Hydrogen spillover in Pd-doped V<sub>2</sub>O<sub>5</sub> nanowires at room temperature. *Chem. Asian J.* 2012;7:684–7.
- [37] Kim BH, Kim A, Oh S-Y, Bae S-S, Yun YJ, Yu HY. Energy gap modulation in V<sub>2</sub>O<sub>5</sub> nanowires by gas adsorption. *Appl. Phys. Lett.* 2008;93:233101.
- [38] Schilling O, Colbow K. A mechanism for sensing reducing gases with vanadium pentoxide films. *Sens. Actuators B* 1994;21:151–7.